Strength functions and spreading widths of simple shell model configurations

Njema Frazier,[1,2] B. Alex Brown,[1,2] and Vladimir Zelevinsky[1,2,3]
[1]*National Superconducting Cyclotron Laboratory, Michigan State University, East Lansing, Michigan 48824-1321*
[2]*Department of Physics and Astronomy, Michigan State University, East Lansing, Michigan 48824-1116*
[3]*Budker Institute of Nuclear Physics, Novosibirsk 630090, Russia*
(Received 25 March 1996)

The exact solution of the many-body problem in the framework of the nuclear shell model with a realistic residual Hamiltonian makes it possible to study the fragmentation of simple configurations as a function of excitation energy and interaction strength. The analysis is performed for 839 states with quantum numbers $J^\pi T=0^+0$ in a system of 12 valence particles within the sd shell. Our statistics allow us to establish the generic shape of the strength function in the region of strong mixing. For the realistic interaction, the strength function is close to Gaussian in the central part and has exponential wings. The spreading width is larger than predicted by the standard golden rule. At the artificially suppressed interaction strength, we recover the Breit-Wigner shape and the golden rule for the spreading width. The transition between these regimes agrees with theoretical considerations based on the idea of chaotic dynamics. [S0556-2813(96)03609-6]

PACS number(s): 21.10.Ma, 21.10.Pc, 21.60.Cs

I. INTRODUCTION

The shell model with semiempirical residual interactions [1,2] is, to date, the most reliable approach to microscopic calculations of nuclear properties. It is especially successful in relatively light nuclei. With the matrix elements of the two-body interactions fitted by the known low-lying levels, it turns out to be possible to reproduce numerous observable quantities in the sd-shell nuclei. Supported by this success, we can move to the region of higher excitation energy and dense level spectrum in order to study the complicated nuclear states which are not accessible individually by experiment. Moreover, it is tempting to extrapolate our findings to other many-body quantum systems with strong interactions between constituents.

As excitation energy and level density increase, the stationary many-body states become exceedingly complicated superpositions of original ''simple'' shell model configurations. The only quantum numbers characterizing a given state are those of exact integrals of motion, angular momentum, parity, and isospin, $J^\pi T$, in our case. In such a situation we expect the new statistical regularities typical for quantum chaos to dominate the dynamics. As we have shown earlier [3–5], the signatures of quantum chaos in the level statistics [6–8] are seen already at weak residual interaction (0.2–0.3 of the actual strength). The nearest level spacing distribution $P(s)$ rapidly reaches the Wigner form. The spectral rigidity $\Delta(L)$ follows the predictions of the Gaussian Orthogonal Ensemble (GOE) up to $L\approx 200$ where it upbends, probably due to the finite bandwidth of the original Hamiltonian matrix related to the selection rules of the two-body interaction. Similar studies have been carried out for heavy atoms [9] as well as for other modifications of the nuclear shell model [10–12].

Local level statistics give the simplest signatures of chaotic dynamics which are not sensitive enough to reveal the deviations from complete chaos in the structure of the many-body eigenfunctions. Using the representation-dependent criteria of information entropy [3,13], we quantified the complexity of the wave functions, discovering that the degree of complexity smoothly evolves along the spectrum, being in fact a weakly fluctuating function of excitation energy. Therefore, it is possible to relate information entropy calculated in the shell model basis to thermodynamic entropy and to the properties of the equilibrium thermal ensemble [4,5]. In an energy window which includes many levels but has an approximately constant level density, the generic wave functions ''look the same'' [14] which justifies the concept of statistical equilibrium.

One of the most important characteristics of the highly excited states is given by the strength function of simple modes. An external field, for example, of electromagnetic nature, acts by a simple one-body operator and excites, in the independent particle shell model, one-particle–one-hole states. In reality, such an excited state is a wave packet of many close stationary states. Each component carries a fraction of the strength of the original simple mode. An experiment with a resolution insufficient for the analysis of the dense fine structure spectrum displays a strength function as an envelope of the strength distribution. Using the language of time evolution, this is interpreted as damping of the simple mode [15], via its decay into complex stationary states. With reasonable statistical assumptions about the nearest level spacing distribution and the strength distribution among the invisible fine structure states, it is possible [16] to reconstruct their level densities and to recover the strength missing in the experiment with poor resolution.

Considering the background of fine structure states as a continuum, one would expect the exponential decay of the original excitation, and, therefore, a Breit-Wigner shape for the strength distribution as a function of the energy distance from the centroid. As known from quantum decay theory, the Breit-Wigner shape which has an infinite second moment cannot be exact [17]. However, it can be a good approximation, except maybe for the extreme wings of the distribution, as shown, for example, for the neutron resonances and giant resonances built on the ground state [18]. A microscopic mechanism for the coupling between the simple mode

and its chaotic environment leading to the Breit-Wigner strength function is explained in detail in [18]. Under assumptions made in this derivation, the width of the distribution is given by the ''golden rule'' in terms of the mean coupling matrix elements and the background level density. We will call this theory a ''standard model.''

At some excitation energy, the spreading width saturates at a level determined by the original matrix elements for the coupling of the simple mode with the doorway states of the next degree of complexity. The saturation of the spreading width is known from the thorough systematics for the isobaric analog resonances [19]. A qualitative explanation of this behavior, using the concepts of chaotic wave functions, was given in [20,21]. Experimental data concerning the dipole giant resonance built on the compound states [22,23] also support the saturation of the spreading width.

The assumptions of the standard model break down when the width Γ_s obtained by the golden rule grows larger than the energy interval ΔE where the background level density and/or the coupling matrix elements can be considered as approximately constant. The existence of this limit of ''strong coupling'' was recognized long ago by Wigner [24] and discussed in the banded random matrix models [25]. The deviations from the standard model are responsible [26,27] for the narrow width of double giant resonances [28]. The formulation of the general approach which contains the standard model and the strong coupling as particular limiting cases was presented in [29].

The goal of the present paper is to study the strength function and the spreading width of simple nuclear configurations in the framework of the realistic shell model. Here we are able to check in detail various statistical hypotheses and to trace the transition between the weak coupling (standard model) and strong coupling situations. At this stage we consider the present work as a numerical experiment testing current theoretical ideas in realistic conditions. We start with a brief review of the standard model and its generalization in Sec. II. The results for the strength function obtained in our shell model are shown in Sec. III. At the realistic interaction strength, the generic shape of the strength function is close to the Gaussian in the central part. Up to high accuracy, the wings are exponential. The spreading width exceeds considerably the golden rule value which can be found with the help of the procedure of excluding a single basis state and considering its coupling to the rest of the system (Sec. IV). The strength function evolves as the interaction is artificially suppressed. In the weak coupling limit, we return to the domain of validity of the standard model and recover the Breit-Wigner shape. Accordingly, the spreading width dependence on the interaction strength changes from linear to quadratic as one proceeds from strong to weak coupling. We conclude with summarizing our results.

II. STRENGTH FUNCTION

A. Definitions

We consider a quantal system governed by the Hamiltonian H and considered in a truncated space spanned by the finite set of the basis states, $|k\rangle$. In this basis, which can be thought of as a traditional basis of the independent particle shell model, the Hamiltonian

$$H = H_0 + H' \tag{1}$$

contains the diagonal configuration energies (which includes both the single-particle and diagonal two-body contributions), given by H_0, and the off-diagonal residual interaction H'. In the actual nuclear diagonalization, the integrals of motion such as total angular momentum (J), parity (π), and isospin (T) are exactly preserved by the projection of the simple shell model Slater determinants (m scheme; see below) so that all states under consideration have the same exact quantum numbers $J^\pi T$.

It is convenient to include the diagonal part of the residual interaction into the unperturbed Hamiltonian. Its eigenfunctions satisfy

$$H_0|k\rangle = \overline{E_k}|k\rangle, \tag{2}$$

where $\overline{E_k} = H_{kk}$. The strict degeneracy of the pure shell model configurations corresponding to a single partition is thereby removed.

By the diagonalization of the full Hamiltonian matrix including the off-diagonal matrix elements H'_{kl}, we obtain the eigenstates $|\alpha\rangle$ and their energies E_α,

$$H|\alpha\rangle = E_\alpha|\alpha\rangle. \tag{3}$$

The eigenstates are the complicated superpositions

$$|\alpha\rangle = \sum_k C_k^\alpha |k\rangle \tag{4}$$

of the basis states. The fragmentation of basis states, $|k\rangle = \Sigma_\alpha C_k^\alpha |\alpha\rangle$, is described by the same transformation coefficients C_k^α which can be taken as real in our case of time reversal invariance. This fragmentation is the object of our studies.

The average characteristics of the fragmentation can be expressed directly in terms of the matrix elements of the Hamiltonian (1). For a given basis state $|k\rangle$, the centroid of the strength distribution coincides with the unperturbed energy (2),

$$\sum_\alpha (C_k^\alpha)^2 E_\alpha = \overline{E_k}. \tag{5}$$

The second moment of the strength distribution is determined by the sum of all off-diagonal matrix elements (starting at a given basis state) squared,

$$\sigma_k^2 \equiv \sum_\alpha (C_k^\alpha)^2 (E_\alpha - \overline{E_k})^2 = \sum_{l \neq k} (H'_{kl})^2. \tag{6}$$

Closely related to, but different from this, is the effective local bandwidth ω_k,

$$\omega_k^2 = \frac{1}{\sigma_k^2} \sum_{l \neq k} (\overline{E_k} - \overline{E_l})^2 (H'_{kl})^2. \tag{7}$$

In contrast to the GOE, the actual shell model Hamiltonian matrix does not couple a state with all others; the two-body interaction leads to the specific selection rules which allow the matrix elements only between configurations which differ in orbits of not more than two particles. This determines the effective bandwidth (7) and brings the matrix closer to

those described by the banded random matrix ensembles (BRME's) [25]. However, our many-body matrix elements are determined by a much smaller number of independent two-body matrix elements and therefore cannot be considered as uncorrelated which is the case in the BRME's. The ensembles based on two-body random interactions in a many-body systems were discussed in [6,30].

All the moments of the strength distribution can be found from the strength function

$$F_k(E)=\sum_\alpha (C_k^\alpha)^2\delta(E-E_\alpha). \tag{8}$$

As compared to the full density of states

$$\rho(E)=\sum_\alpha \delta(E-E_\alpha), \tag{9}$$

the strength function (8) is frequently called the ''local density of states.'' It determines the contribution of the basis state $|k\rangle$ to $\rho(E)$ at $E=E_\alpha$,

$$F_k(E)=\rho(E)\langle (C_k^\alpha)^2\rangle_{E_\alpha=E}. \tag{10}$$

Equation (10) assumes that the strength function is approximated by the histogram where we sum in Eq. (8) over the eigenstates within a narrow energy bin which contains, due to the high level density, many states of close degree of complexity.

Our functions are normalized according to

$$\int dE\rho(E)=N, \quad \int dEF_k(E)=1. \tag{11}$$

Here N is the total dimension of Hilbert space.

B. Standard model

In the standard derivation of the strength function [18], one singles out a state $|k\rangle$ which is initially removed from the Hamiltonian matrix. The diagonalization of the remaining $(N-1)\times(N-1)$ matrix gives the intermediate ''background'' states $|\nu\rangle$, their eigenvalues e_ν, and wave functions $|\nu\rangle=\Sigma_{k'\neq k}\langle k'|\underline{\nu}\rangle|k'\rangle$. The full matrix expressed in the basis $(|k\rangle,\{|\nu\rangle\})$ has E_k and intermediate energies e_ν on the main diagonal and off-diagonal matrix elements

$$V_{k\nu}=V_{\nu k}=\sum_{k'\neq k} H'_{kk'}\langle k'|\nu\rangle \tag{12}$$

due to the coupling between the single state $|k\rangle$ and the background. The advantage of this approach is that the omission of a single state cannot change significantly the statistical properties of the dense spectrum. We can expect that the level density of the background is the same as in the exact solution including all N states.

The problem of the interaction of the single state with the background can be easily solved. The eigenstates $|\alpha\rangle$ are the combinations

$$|\alpha\rangle=C_k^\alpha|k\rangle+\sum_\nu B_\nu^\alpha|\nu\rangle, \tag{13}$$

where the amplitudes C_k^α coincide with those in Eq. (4). Eliminating the coefficients B_ν^α with the use of the Schrödinger equation and normalizing the wave function, we obtain

$$(C_k^\alpha)^2=\left[1+\sum_\nu \frac{V_{k\nu}^2}{(E_\alpha-e_\nu)^2}\right]^{-1}. \tag{14}$$

The exact eigenvalues E_α are the poles of the Green function $G(E)=(E-H)^{-1}$ or the roots of the secular equation

$$E_\alpha-\overline{E_k}-\sum_\nu \frac{V_{k\nu}^2}{E_\alpha-e_\nu}=0, \tag{15}$$

whereas the weights (14) are the corresponding residues of $G(E)$. The roots (15) do not depend on the original choice of the excluded state $|k\rangle$. These equations do not contain any approximation.

The results of the standard model are based on additional assumptions.

(i) The background spectrum is dense and rigid, and so one can consider instead an equidistant sequence of levels with the mean spacing D.

(ii) The coupling intensities $V_{k\nu}^2$ are uncorrelated with the energies e_ν of the background states and weakly fluctuate around the mean value $\langle V^2\rangle$.

(iii) The mixing is sufficiently strong, $\langle V^2\rangle/D^2>1$.

Under these assumptions, it is easy to calculate the sums over the intermediate states ν and to obtain the strength function (10) of Breit-Wigner shape,

$$F_k(E)=\frac{1}{2\pi}\frac{\Gamma_s}{(E-E_k)^2+\Gamma_s^2/4}, \tag{16}$$

with the spreading width Γ_s given by the golden rule

$$\Gamma_s=2\pi\frac{\langle V^2\rangle}{D}. \tag{17}$$

Expressions (16) and (17) are sometimes taken for granted although they are valid under above-mentioned assumptions only. We note also that we use here the term ''golden rule'' for the spreading width (17) with no relation to perturbation theory. This result is valid in the domain of validity of the standard model.

C. General description and strong coupling limit

As discussed in [5], the assumptions of the standard model are correct as long as the resulting standard spreading width is relatively small. Γ_s should be compared with the energy range ΔE within which the level density and the coupling matrix elements can be considered as approximately constant. In the framework of the shell model, the two-body interactions are capable of admixing the close configurations of gradually increasing level of complexity. They serve as the doorway states for the further process of stochastization. The doorway states have their own spreading width which determines the energy range for effective mixing of the origi-

nal state. The finiteness of this energy interval plays no role if $\Gamma_s < \Delta E$. The formal limit of $\Delta E \to \infty$ corresponds to the standard model.

As the coupling strength and the spreading width increase, the finite size of the doorway strength interval becomes important. One can estimate what happens in this limit assuming that the coupling $\underline{V}^2_{k\nu}$ suddenly disappears at some finite distance $\Delta E = e_\nu - \overline{E}_k$ from the centroid $\overline{E}_k$. A mean value of this interval can be inferred from the ''bandwidth'' ω_k, Eq. (7). The strength distribution is then determined by the outer roots of the secular equation (15) which are located well outside of the bandwidth at the distance

$$(E_\alpha - \overline{E_k})^2 = \sum_\nu V^2_{k\nu} = \sigma^2_k, \tag{18}$$

where the last equality follows from the definition (6), expression (12) for the transformed coupling matrix elements, and the completeness of the set of the intermediate states $|\nu\rangle$ in space of dimension $(N-1)$.

Thus, the result (18) allows one to give a simple estimate

$$\Gamma_k \approx 2\sigma_k \tag{19}$$

for the spreading width in the limit of complete mixing. Written as Eq. (19), the expression for the spreading width does not refer to the specific form of decrease of the coupling matrix elements $V_{k\nu}$ as one moves away from the centroid $\overline{E}_k$. Using the idea of similarity of complicated states in a given energy region [29,5], we expect small variations of the width for various states $|k\rangle$ in this limit. Indeed, the quantity σ_k found for the sd-shell model is roughly constant for nearly all states.

The new and important property of the strong coupling limit (19) is that the quadratic dependence of the spreading width on the interaction strength is replaced by the linear dependence. Such a prediction was first made on qualitative grounds [26] in relation to the problem of the damping width of the double giant resonances. In the harmonic approximation for the giant mode, the matrix elements $V_{k\nu}$ of the coupling between the collective n-phonon state $|k\rangle$ and the compound states $|\nu\rangle$ scale as $\sqrt{n}$. Therefore, in agreement with data [28], the ratio $\Gamma(n)/\Gamma(1)$ of the widths of the multiple and single excitations should increase $\propto \sqrt{n}$ in the strong coupling limit (19) rather than $\propto n$ as predicted by the golden rule (17) with the quadratic dependence on the coupling matrix elements. The transition is nicely reproduced in numerical simulations [27].

To understand the underlying mechanism leading to the linear dependence of the spreading width, one can refer to the N scaling of the matrix elements [31,32] occurring as one proceeds to the mixed states at high excitation energy and high density. At a stage of the mixing process when a complicated state (4) contains N significant simple basis components $|k\rangle$, the matrix elements V between this state and one of simple states are reduced in average by factor $N^{-1/2}$ compared to typical matrix elements v between original simple states. The coupling intensity $\langle V^2 \rangle$ at this degree of complexity can be estimated as v^2/N. The quantity ND in the denominator of Eq. (17) gives the order of magnitude of the energy range covered by the fragmented strength of the original state. Thus, it is proportional to the spreading width, and the self-consistent consideration of Eq. (17) gives $\Gamma \propto v$, i.e., the linear dependence on the interaction strength. Beyond this point, the regime of strong coupling takes place where the saturation of the spreading width as a function of excitation energy is expected.

The detailed behavior of the spreading width as a function of the interaction strength depends on the explicit dependence of the level density and the coupling matrix elements on the energy of the background states. The general theory which incorporates this behavior as input and then predicts the strength function and the value of the spreading width was developed in [29]; see also [5]. When going from weak to strong coupling, the strength function evolves from the Breit-Wigner form, Eq. (16), to the nonuniversal shape with a finite second moment. The spreading width [defined as the full width at half maximum (FWHM)] undergoes a transition from the quadratic dependence of the standard golden rule to the linear dependence, similar to our estimate (19). However, the form of theory suggested in [29] assumes the uniformity of the statistical properties of all complicated states. This assumption is not completely valid in our case because the wide strength functions at the realistic interaction stength cover the regions with quite different degrees of complexity.

Since the specific features of the results for the shell model residual interaction should be shown below, at this point we limit ourselves with the simple interpolation formula for the spreading width as a function of the strength of the residual interaction λ,

$$\Gamma = \frac{\gamma \lambda^2}{1 + y\lambda}. \tag{20}$$

Foreseeing that in the region of chaotic dynamics one can define a generic strength function of the basic states, we omit here the basis state label k. Of course, there can be fluctuations of the spreading width from one basis state to another one. The case of the collective state with a nongeneric strength function was studied in [29]. The scale λ is defined as a common factor in front of the residual off-diagonal interaction H' in (1); $\lambda = 1$ corresponds to the realistic strength.

The parameters γ and y of Eq. (20) are related to the weak and strong coupling limits. For the weak interaction case, the comparison of Eqs. (17) and (20) determines

$$\gamma = \frac{2\pi}{D_0} \frac{\langle V^2(\lambda) \rangle}{\lambda^2}, \tag{21}$$

where D_0 is the mean level spacing for the unperturbed system. The strong coupling limit determines, according to Eq. (19),

$$1 + y = \frac{\gamma}{2\overline{\sigma}} \approx \frac{\pi \langle V^2 \rangle}{D_0 \overline{\sigma}}, \tag{22}$$

where $\langle V^2 \rangle$ and the mean value $\overline{\sigma}$ of the quantity (6) are taken at $\lambda = 1$ under the assumption that the actual value of the interaction strength belongs to the chaotic regime.

III. STRENGTH FUNCTIONS OF SHELL MODEL STATES

A. Model

The modern nuclear shell model provides an exact solution of the quantum many-body problem within a truncated space of several nucleon configurations. The space dimensions of the order of 10^3 are easy to handle. On the other hand, they are sufficiently large to make the results statistically reliable. We use the Wildenthal Hamiltonian [1] which defines the single-particle energies and the interaction between the valence particles by fitting more than 400 binding energies and excitation energies for the sd-shell nuclei. In this paper we carry out calculations exclusively for the $J^\pi T = 0^+0$ states of 12 particles above the inert core of ^{16}O. The system can be considered as a model for the ^{28}Si nucleus in the approximation when the interaction across the major shells is neglected. Examples of other shell model applications for similar purposes can be found in [5].

The 0^+0 class contains $N = 839$ states. They are partitioned into shell model configurations according to the occupation numbers of the spherical orbits $0d_{5/2}, 0d_{3/2}$, and $1s_{1/2}$. The calculations are carried out with the OXBASH code [2]. The original configurations are described in the m scheme. This requires, as a prerequisite for the diagonalization, the construction, with the help of the projection operators, of the proper linear combinations of the m states within a partition which have the desired values $J^\pi T$. These superpositions are the basis states $|k\rangle$ of Eq. (2). As discussed in [5], the projection procedure already creates fairly complex nondeterminantal states which still have very close bare energies $\overline{E_k}$.

There are 63 independent two-body interaction matrix elements which define all many-body matrix elements. The latter therefore cannot be considered uncorrelated as in the GOE or BRME's. The global properties of the mixing interaction are seen [5] by inspection of the matrix H' prior to the actual diagonalization. The second moment σ_k, Eq. (6), and the effective bandwidth ω_k, Eq. (7), both stay essentially constant for the majority of the states $|k\rangle$. Their fluctuations are presumably of statistical character. The mean values of these quantities for the 0^+0 states are $\overline{\sigma} \approx 10$ MeV and $\overline{\omega} \approx 8$ MeV. The constancy of σ_k is one of the manifestations of the N scaling [31,32]: As the mixing proceeds involving the increasing number N of fine structure states, each coupling matrix element diminishes $\propto 1/\sqrt{N}$, keeping the sum (6) constant. The same phenomenon is responsible for the saturation of the damping width of giant resonances [22,23] and isobaric analog resonances [20,21].

The direct diagonalization of the Hamiltonian matrix results in the energies E_α of the eigenstates $|\alpha\rangle$ and their wave functions expressed as the superpositions (4) of the basis states. The level density (9) has a Gaussian shape with the variance which is equal to $\sigma_E^0 = 8$ MeV without the off-diagonal interaction ($\lambda = 0$). The variance broadens up to $\sigma_E = 13$ MeV at $\lambda = 1$. The mean level spacings near the middle of the spectrum are $D_0 = 24$ keV and $D = 40$ keV for $\lambda = 0$ and $\lambda = 1$, respectively. It is known [6,33] that the Gaussian shape occurs mainly due to combinatorial reasons for the two-body interaction in the many-body system, irrespective of the random or deterministic (as in our case) nature of the two-body matrix elements. In contrast, the Wigner semicircle level density is obtained for the uncorrelated many-body matrix elements in a full or banded (but sufficiently wide) matrix.

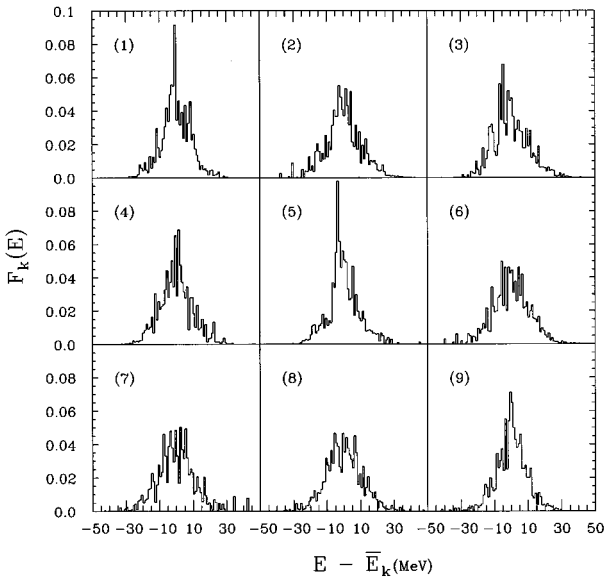

FIG. 1. The strength functions for nine individual 0^+0 basis states $|k\rangle$ in the middle of the spectrum (histograms) vs the energy distance $E - \overline{E_k}$ from the centroid of the unperturbed state $|k\rangle$, panels 1–9. The bin size is 1 MeV.

We refer the reader to the review paper [5] for a detailed study of the chaotic properties of the 0^+0 states. The local level statistics (the nearest level spacing distribution and the spectral rigidity) display an onset of chaos already for the weak interaction, $\lambda \approx 0.2$. The complexity of the eigenstates and related localization length measured in the original basis continues to regularly evolve beyond this point. This manifests the greater sensitivity of the wave functions to the deviations from the chaotic limit. Below we concentrate on the structure of the individual eigenstates which will allow us to extract the generic strength function.

B. Shape of the strength function

One of the main conclusions of the analysis given in [5] was that of the similarity of individual wave functions in the chaotic region, in accordance with Percival's conjecture [14]. The degree of complexity of the eigenstates, measured by information entropy and/or by the moments of the distribution function of the amplitudes C_k^α was found to saturate in the central part of the spectrum. The average properties of the eigenstates with approximately the same degree of complexity can be related to thermodynamical entropy and temperature of the equilibrium thermal ensemble [4]. These properties can be extracted by averaging out the fluctuations.

We expect that the closely related problem of the fragmentation of the basis states over the eigenstates can be solved similarly. Figure 1 shows the ''empirical'' strength functions $\underline{F_k}(E)$, Eq. (10), for nine basis states $|k\rangle$ with the centroids E_k located in the middle of the spectrum. The histograms obtained with the bin size of 1 MeV are plotted as a function of the energy distance from the corresponding centroid. Taking the basis states in this high-density mid-energy

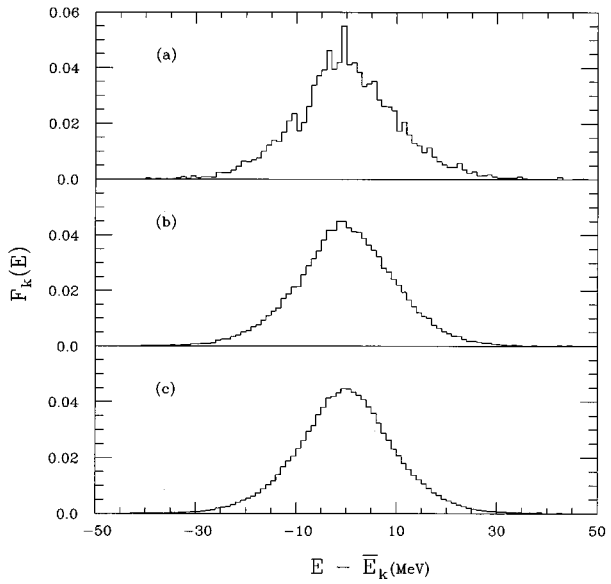

FIG. 2. The strength function averaged over 10, 100, and 400 0^+0 states in the middle of the spectrum, panels (a)–(c), respectively. The bin size is 1 MeV.

region as members of a statistical ensemble, we superimpose their strength functions in order to reduce the statistical fluctuations and produce a smooth, ''generic'' strength function. In Fig. 2 this averaging, with the same bin size, is performed over 10, 100, and 400 basis states, parts (a), (b), and (c), respectively.

The resulting strength function is already very smooth at the step (b). The wings of the curve are decreasing much faster than expected for the Breit-Wigner distribution (16). For the detailed fit we use the histograms with the finer bin size of 100 keV. Figure 3 demonstrates that the Breit-Wigner

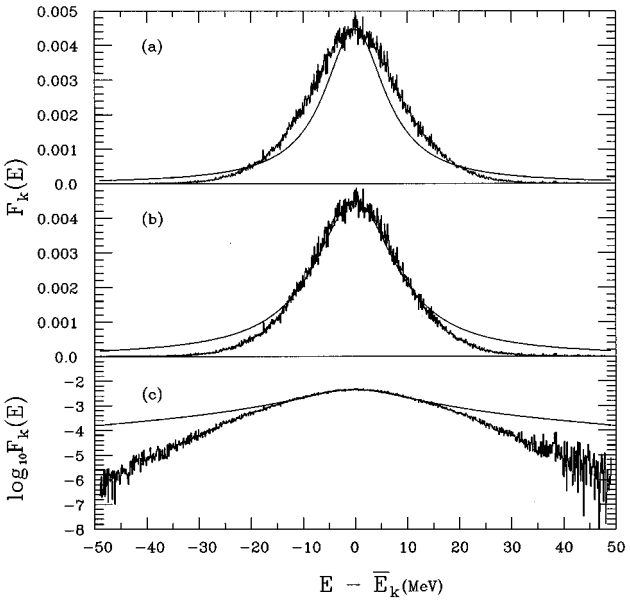

FIG. 3. The overall Breit-Wigner fit (solid lines) to the strength function of Fig. 2(c) (histograms), panel (a), to the central part of the strength function of Fig. 2(c) (histograms), panel (b), and the same fit on the logarithmic scale, panel (c). The bin size is 100 keV.

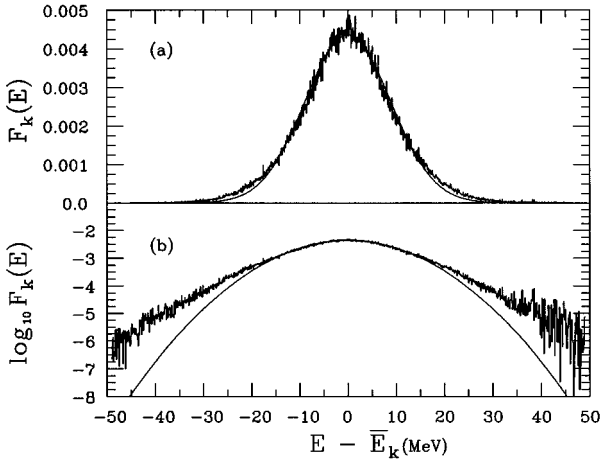

FIG. 4. The Gaussian fit (solid lines) to the strength function of Fig. 2(c) (histograms), panel (a), and the same fit on the logarithmic scale, panel (b). The bin size is 100 keV.

curve does not fit particularly well in any region [Fig. 3(a)]. Our attempt, Fig. 3(b), to fit only the central region results in an extremely poor fit to the tails, Fig. 3(c). Together with the width exceeding the quantity $\overline{\omega}$, this means that the strong coupling case is closer to reality for the states in the middle of the spectrum at the actual interaction strength.

The overall Gaussian fit, Fig. 4(a), is better. With the variance obtained from the Gaussian fit, $\sigma_F = 8.9 \pm 0.7$ MeV, the typical spreading width (FWHM) of the central 0^+0 states equals $\Gamma = (8\ln 2)^{1/2}\sigma_F = 21$ MeV. This agrees with the estimate (19), $\Gamma = 2\overline{\sigma} = 20$ MeV, made for the strong coupling limit. We again observe deviations from the Gaussian shape in the tails of the strength function, Fig. 4(b).

Because of the breakdown of both the Gaussian and the Breit-Wigner fits for the tails of the strength function, it becomes necessary to examine both the central region and the tails of the distribution more closely. According to Eq. (10), the strength function histograms actually involve two factors, the average value $\langle (C_k^\alpha)^2 \rangle$ of the eigenfunction components corresponding to the basis state $|k\rangle$ and the level density $\rho(E)$. The level density itself is described [5] by the Gaussian curve of Fig. 5. This is typical [6] for many-body systems with two-body interactions in the finite Hilbert space. The level density effects dominate the central part of the strength function. Eliminating the level density from the strength function, we come to the ''pure'' weight function $\langle (C_k^\alpha)^2 \rangle$ of Fig. 6.

We see that the Breit-Wigner shape that fits poorly to the strength function [Fig. 3(a)] is noticeably improved in the central region for the pure weight function of Fig. 6(a). The tail of the weight distribution on a logarithmic scale shows a linear behavior, Fig. 6(b). It is clear from Fig. 7, especially from the logarithmic plot of Fig. 7(b), that such an exponential fit does, in fact, represent the tails of the strength distribution. The final form of this fit is

$$F_k(E - \overline{E_k}) \approx F_0 \exp\left(- \frac{E - \overline{E_k}}{E_l} \right), \tag{23}$$

where the energy localization length is $E_l = 5$ MeV. Of course, the expression (23) is valid only for the tails of the

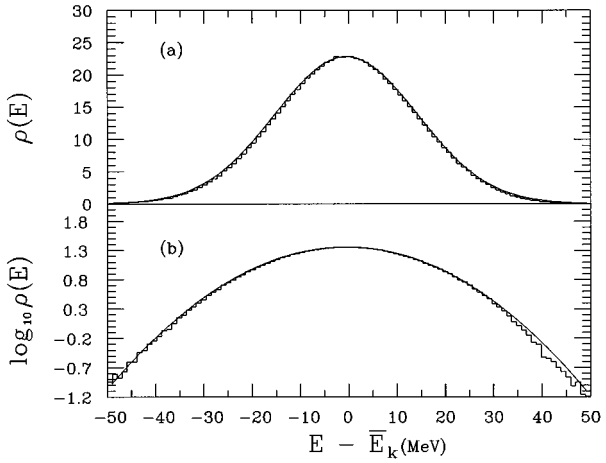

FIG. 5. Gaussian fit (solid lines) to the level density, $\rho(E)$, for the strength function averaged over 400 states, panel (a), and the same fit on the logarithmic scale, panel (b). The bin size is 1 MeV.

distribution, $(E-\overline{E_k})>\Gamma$. The exponential behavior holds for at least three orders of magnitude.

A strength function falling off much faster than the Breit-Wigner distribution was also seen, with larger numerical uncertainty, in a study of atomic levels [9] where several interpolating formulas connecting the middle and the wings of the curve were suggested. The exponential localization is the part of the folklore accompanying studies of complicated wave functions [13]. To the best of our knowledge, the general proof of this notion is missing. The exponential localization of the wave functions in real space is known [34] in disordered solids. The situation in this case is different because the localized functions of nearly the same energy do not overlap if the distance between their centroids exceeds the spatial size of the wave function. In the limit of large N, these functions do not interact, which implies level statistics of the Poisson type. In our case, the exponential wings of the strength function coexist with the perfect chaotic level statistics.

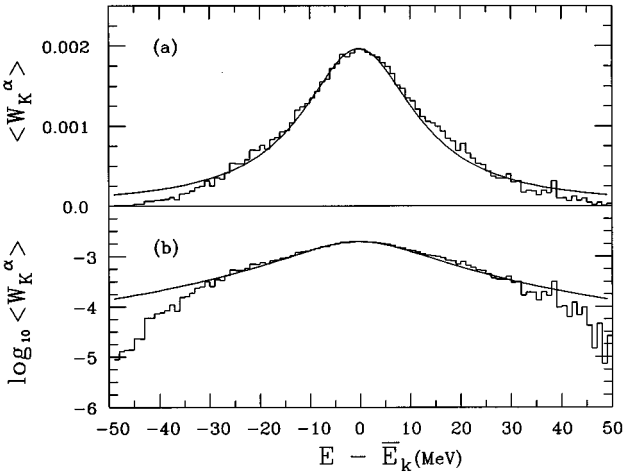

FIG. 6. Breit-Wigner fit (solid lines) to the average weight, $\langle W_k^\alpha\rangle=\langle(C_k^\alpha)^2\rangle$, for 400 states, panel (a), and the same fit on the logarithmic scale, panel (b). The bin size is 1 MeV.

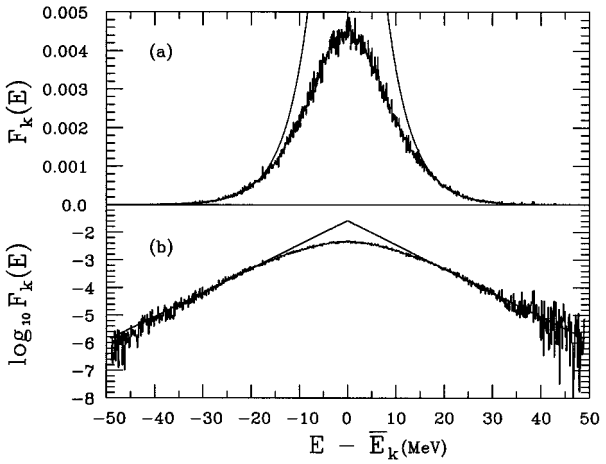

FIG. 7. The exponential fit of Eq. (23), solid lines, to the wings of the strength function of Fig. 2(c) (histograms), panel (a), and the same fit on the logarithmic scale, panel (b). The bin size is 100 keV.

IV. SPREADING WIDTH

A. Two-step diagonalization and the spectral function

In order to observe the spreading widths of individual shell model states, we performed the procedure of the two-step diagonalization described earlier in relation to the standard model. Taking out an arbitrary basis state $|k\rangle$ and performing the diagonalization of the remaining matrix we obtain the intermediate basis $(|k\rangle,\{|\nu\rangle\})$ with energies $(\overline{E_k},\{e_\nu\})$ and coupling matrix elements $V_{k\nu}$, Eq. (12), between the single excluded state and intermediate fine structure states. As we discussed, in the realistic situation these matrix elements are correlated with the energy distance $\overline{E_k}-e_\nu$. To characterize the distribution function of the coupling matrix elements, we introduce, for each removed state $|k\rangle$, the spectral function (form factor)

$$g_k(\overline{E_k},\overline{E_k}+\omega)=\sum_\nu |V_{k\nu}|^2\delta(\overline{E_k}-e_\nu+\omega). \tag{24}$$

This function can be presented by a histogram with the help of the density $\overline{\rho_k}(e_\nu)$ of the intermediate states available for the mixing with the single state $|k\rangle$. Introducing the average coupling intensity $\langle|V_{k\nu}|^2\rangle$, we get, for the spectral form factor (24),

$$g_k(\overline{E_k},\overline{E_k}+\omega)\approx\overline{\rho_k}(\overline{E_k}+\omega)\langle|V_{k\nu}|^2\rangle. \tag{25}$$

According to Eq. (18), this function is normalized as

$$\int d\omega g_k(\overline{E_k},\overline{E_k}+\omega)=\sigma_k^2. \tag{26}$$

Using the same arguments of uniform complexity, we expect to be able to extract the ''generic'' spectral function $\overline{g(\omega)}$, depending on the transition frequency ω only, from the superposition of the form factors g_k derived for different original states $|k\rangle$.

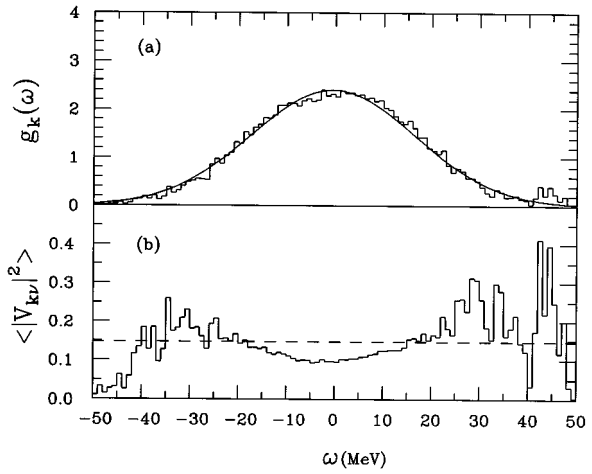

FIG. 8. (a) The spectral form factor $g(\omega)$ averaged over 100 0^+0 basis states in the middle of the spectrum, (histograms); Gaussian fit (solid line). (b) The coupling intensity $\langle V_{k\nu}^2 \rangle$ for the same basis states $|k\rangle$ in the middle of the spectrum (histogram), as a function of $\omega = e_\nu - \overline{E_k}$; dashes correspond to the constant value of $\langle V^2 \rangle = 0.149$ MeV^2.

As the interval of averaging increases, the average form factor rapidly evolves into the Gaussian shape. The form factor averaged over 100 close states is shown in Fig. 8(a) together with the Gaussian fit. The dispersion of the Gaussian is equal to $\sigma_g = 17$ MeV. The fitted normalization leads to the integral $\int d\omega \overline{g(\omega)} = 104$ MeV^2 which agrees [see Eq. (26)], with the average value of $\sigma_k \approx \overline{\sigma} \approx 10$ MeV.

Dividing out the level density of the intermediate basis states, we determine, Fig. 8(b), the average coupling intensity $\langle |V_{k\nu}|^2 \rangle$, Eq. (25). Except for the excess corresponding to the highest and, less pronounced, lowest states $|\nu\rangle$, the matrix elements are nearly constant on the level $\langle |V|^2 \rangle \simeq 0.149$ MeV^2. This means that the realistic coupling is strong and it involves the remote parts of the spectrum with a different level density which mainly determines the shape of the form factor.

The value of the average coupling strength substituted into the golden rule (17) along with the average level spacing ~ 100 keV would result in the spreading width $\Gamma \approx 9.4$ MeV which is less than the value of 21 MeV found directly from the data by a factor of 2.2. The evident disagreement demonstrates that the golden rule estimate based on the standard model is not reliable when dealing with fragmentation and spreading widths which are of the order or larger than the scale of the change of the level density. Taking, instead of the average level density, the significantly larger level density in the center of the spectrum, $D \approx 40$ keV, we would get the golden rule width of 23 MeV, which is closer to the actual value.

Finally, we show in Fig. 9 that, in the intermediate basis, the wings of the strength function $F_k(E)$ can be actually calculated by perturbation theory using in Eq. (10) the weight coefficients

$$\langle (C_k^\alpha)^2 \rangle \rightarrow (C_k^\nu)^2 \equiv \left(\frac{V_{k\nu}}{\overline{E_k} - e_\nu} \right)^2 . \tag{27}$$

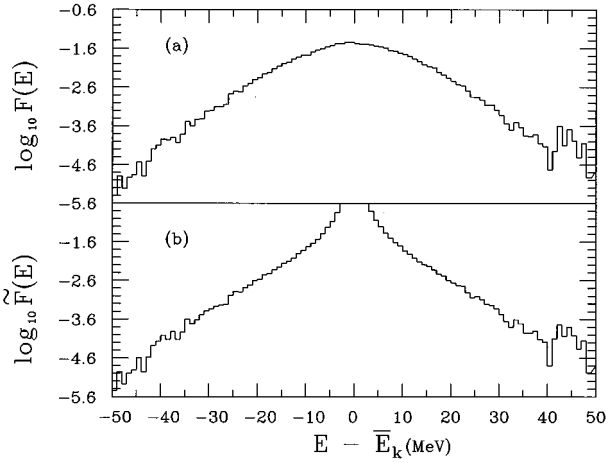

FIG. 9. Strength function $F_k(E)$, panel (a), and perturbative result $\widetilde{F}_k(E)$, panel (b), on a logarithmic scale. Bin size is 1 MeV.

The agreement with the original calculation in the peripheral region is seen by coincidence of the two logarithmic plots.

B. Dependence on the interaction strength

Here we study the evolution of the strength function and the spreading width as a function of the strength of the residual interaction λ. As we mentioned, the level statistics reveal standard signatures of quantum chaos already at $\lambda \approx 0.2$. The mixing of the wave functions, the growth of the degree of complexity, and the evolution of the strength function are parallel aspects of the stochastization process.

In agreement with the general trends discussed in Sec. II, at weak interaction strength the shape of the strength function becomes closer to the Breit-Wigner one. Figure 10 clearly shows the Breit-Wigner behavior for $\lambda = 0.1, 0.2$, and 0.3, panels (a), (b), and (c), respectively. The whole evolution pattern is seen in the logarithmic plots of Figs. 11 and

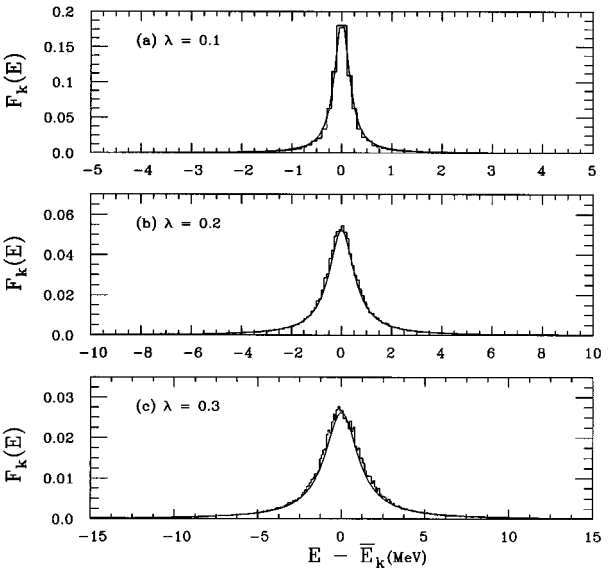

FIG. 10. Breit-Wigner fit (solid lines) to the strength function averaged over 400 0^+0 midenergy states for $\lambda = 0.1$, 0.2, and 0.3, panels (a), (b), and (c), respectively. The bin size is 100 keV.

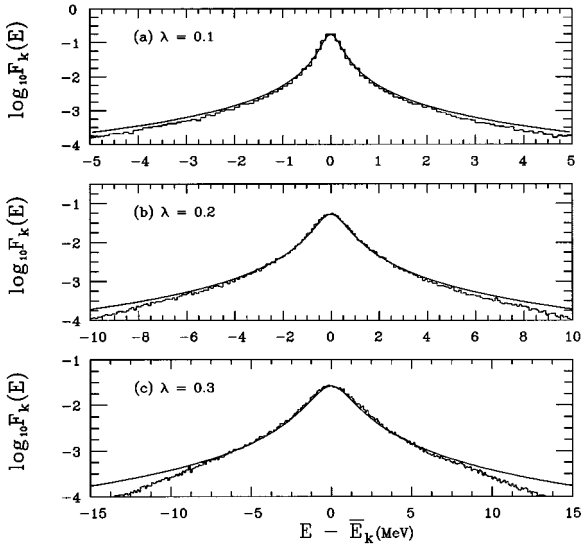

FIG. 11. Breit-Wigner fit (solid lines) to the strength function averaged over 400 0^+0 mid-energy states for $\lambda = 0.1$, 0.2, and 0.3, panels (a), (b), and (c), respectively, on a logarithmic scale. The bin size is 100 keV.

12. The curve evolves in the direction of the Gaussian in the central part with exponential tails. The Breit-Wigner description of the main part of the strength function can be considered as satisfactory up to $\lambda \approx 0.4$. In this region the narrow strength function is not strongly influenced by the change of the level density. As seen from Fig. 13, the quality of the Gaussian fit clearly improves as one goes to the strong coupling limit; the last panel, (d), corresponds to $\lambda = 1.2$.

Using ''empirical'' generic strength functions, we can trace the evolution of the spreading width (FWHM) as a function of the intensity of the residual interaction. Figure 14 shows the results for the values of λ between 0 and 1.2. The

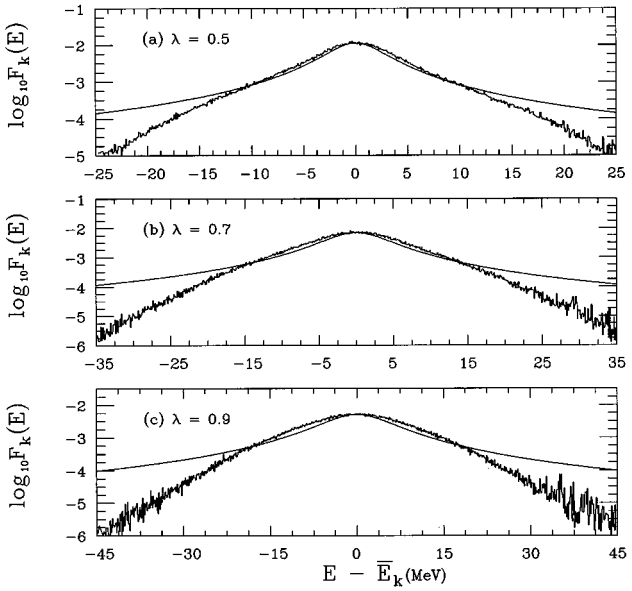

FIG. 12. Breit-Wigner fit (solid lines) to the strength function averaged over 400 0^+0 mid-energy states for $\lambda = 0.5$, 0.7, and 0.9, panels (a), (b), and (c), respectively, on a logarithmic scale. The bin size is 100 keV.

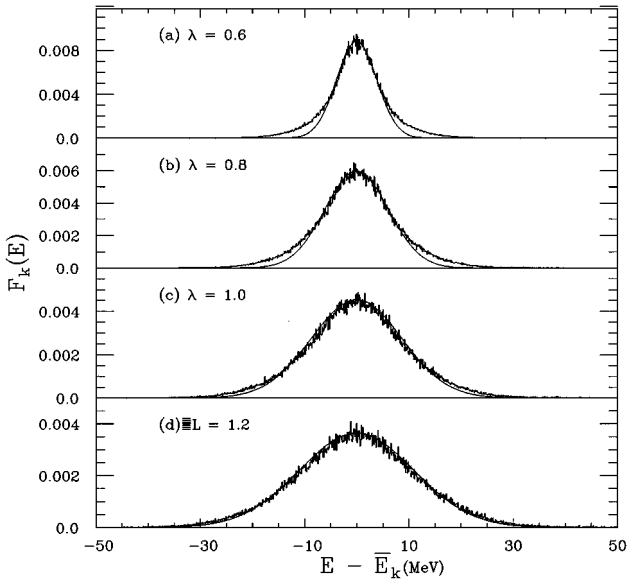

FIG. 13. Gaussian fit to the strength function averaged over 400 0^+0 mid-energy states for $\lambda = 0.6$, 0.8, 1.0, and 1.2, panels (a), (b), (c), and (d), respectively.

dependence of the spreading width on the interaction changes from quadratic in the weak coupling limit to linear at strong coupling. The results are nicely described by the simple interpolation (20) with parameters $\gamma \approx 44.9$ MeV and $y \approx 1.32$. Our estimates (21) and (22), using the value of the average level spacing at weak interaction $D_0 \approx 21$ keV, predict for these parameters $\gamma = 44.6$ MeV and $y = 1.23$.

V. CONCLUSION

The typical strength function for stationary nuclear states was, for the first time, extracted from the exact solution of the many-body problem in the truncated Hilbert space of

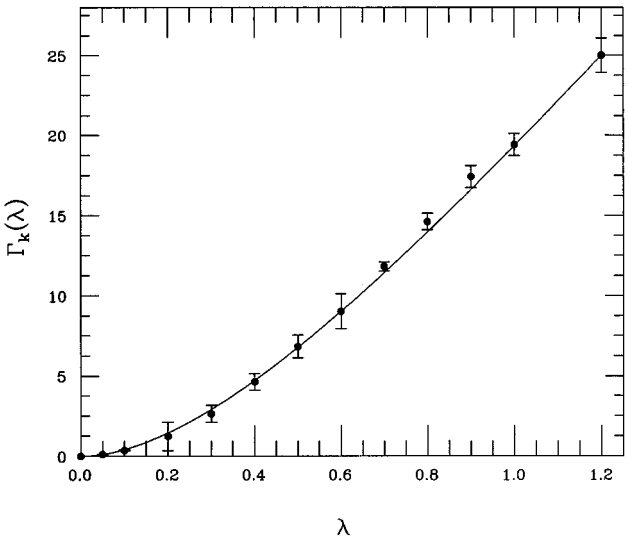

FIG. 14. Spreading width Γ_k of the basis states as a function of the interaction strength λ for 400 middle 0^+0 states. The solid line corresponds to Eq. (20) with $\gamma = 44.9$ MeV and $y = 1.32$. The error bars are defined by the deviations of the fit from the calculated data.

shell model configurations. The realistic interaction strength corresponds to the strong coupling case which cannot be satisfactorily described by the standard model of the strength function. The generic shape of the compound states at high excitation energy is close to a Gaussian but with exponential wings. At this point we cannot explain the factor responsible for the exponential localization length. In order to better understand this we should investigate the strength function evolution along the spectrum; here, we studied the most complicated states near the middle which could be considered as uniform in their properties including the shape and the width of the strength function.

The transition to the weak coupling case at the artificially suppressed strength of the residual interaction shows how the shape of the strength function regularly changes from the Gaussian to the ''normal'' Breit-Wigner. This is accompanied by the reduction of the spreading width and the smooth transition from the linear interaction dependence characteristic for the strong coupling limit to the ordinary quadratic dependence predicted by the golden rule. This transition is seen for the first time in realistic calculations.

New effects will enter when the presence of real decay into continuum is taken into account. The competition of the internal mixing, external decay, and interaction through common decay channels makes the whole problem more complicated. This interplay of various mechanisms will determine the physics of compound states at high excitation energy in stable nuclei and at lower excitation energy in weakly bound nuclei.

The authors acknowledge support from NSF Grants Nos. 94-03666 and 95-12831.

[1] B.A. Brown and B.H. Wildenthal, Annu. Rev. Nucl. Part. Sci. **38**, 29 (1988).
[2] B.A. Brown *et al.*, OXBASH, MSUNSCL Report No. 524, 1988.
[3] V. Zelevinsky, M. Horoi, and B.A. Brown, Phys. Lett. B **350**, 141 (1995).
[4] M. Horoi, V. Zelevinsky, and B.A. Brown, Phys. Rev. Lett. **74**, 5194 (1995).
[5] V. Zelevinsky, B.A. Brown, N. Frazier, and M Horoi, Phys. Rep. (to be published).
[6] T.A. Brody, J. Flores, J.B. French, P.A. Mello, A. Pandey, and S.S.M. Wong, Rev. Mod. Phys. **53**, 385 (1981).
[7] O. Bohigas and H.A. Weidenmüller, Annu. Rev. Nucl. Part. Sci. **38**, 421 (1988).
[8] F. Haake, *Quantum Signatures of Chaos* (Springer, New York, 1991).
[9] V.V. Flambaum, A.A. Gribakina, G.F. Gribakin, and M.G. Kozlov, Phys. Rev. A **50**, 267 (1994).
[10] B.A. Brown and G.F. Bertsch, Phys. Lett. **148B**, 5 (1984).
[11] W.E. Ormand and R.A. Broglia, Phys. Rev. C **46**, 1710 (1992).
[12] S. Drożdż, S. Nishizaki, J. Speth, and J. Wambach, Phys. Rev. C **49**, 867 (1994).
[13] F.M. Izrailev, Phys. Rep. **196**, 299 (1990).
[14] I.C. Percival, J. Phys. B **6**, L229 (1973).
[15] G.F. Bertsch, P.F. Bortignon, and R.A. Broglia, Rev. Mod. Phys. **55**, 287 (1985).
[16] G. Kilgus *et al.*, Z. Phys. A **326**, 41 (1987).
[17] P.M. Gopych *et al.*, Sov. J. Part. Nucl. **19**, 338 (1988).
[18] A. Bohr and B. Mottelson, *Nuclear Structure* (Benjamin, New York, 1969), Vol. 1.
[19] J. Reiter and H.L. Harney, Z. Phys. A **337**, 121 (1990).
[20] H.L. Harney, A. Richter, and H.A. Weidenmüller, Rev. Mod. Phys. **58**, 607 (1986).
[21] V.G. Zelevinsky and P. von Brentano, Nucl. Phys. **A529**, 141 (1991).
[22] A. Bracco *et al.*, Phys. Rev. Lett. **62**, 2080 (1989); G. Enders *et al.*, *ibid.* **69**, 249 (1992); J.J. Gaardhøje, Annu. Rev. Nucl. Part. Sci. **42**, 483 (1992).
[23] A. Bracco *et al.*, Phys. Rev. Lett. **74**, 3748 (1995).
[24] E.P. Wigner, Ann. Math. **62**, 548 (1955).
[25] M. Feingold, A. Gioletta, F.M. Izrailev, and L. Molinari, Phys. Rev. Lett. **70**, 2936 (1993).
[26] C.A. Bertulani and V.G. Zelevinsky, Phys. Rev. Lett. **71**, 967 (1993); Nucl. Phys. **A568**, 931 (1994).
[27] C.H. Lewenkopf and V.G. Zelevinsky, Nucl. Phys. **A569**, 183 (1994).
[28] S. Mordechai *et al.*, Phys. Rev. C **41**, 202 (1990); J. Ritman *et al.*, Phys. Rev. Lett. **70**, 533 (1993); R. Schmidt *et al.*, *ibid.* **70**, 1767 (1993); T. Aumann *et al.*, Phys. Rev. C **47**, 1728 (1993).
[29] B. Lauritzen, P.F. Bortignon, R.A. Broglia, and V. Zelevinsky, Phys. Rev. Lett. **74**, 5190 (1995).
[30] V.V. Flambaum, G.F. Gribakin, and F.M. Izrailev, Phys. Rev. E **53**, 5729 (1996).
[31] O.P. Sushkov and V.V. Flambaum, Pis'ma Zh. Éksp. Teor. Fiz. **32**, 377 (1980) [JETP Lett. **32**, 353 (1980)]; Usp. Fiz. Nauk **136**, 3 (1982) [Sov. Phys. Usp. **25**, 1 (1982)].
[32] V.G. Zelevinsky, Nucl. Phys. **A553**, 125c (1993); **A570**, 411c (1994).
[33] K.K. Mon and J.B. French, Ann. Phys. (N.Y.) **95**, 90 (1975).
[34] I.M. Lifshits, S.A. Gredescul, and L.A. Pastur, *Introduction to the Theory of Disordered Systems* (Wiley, New York, 1988).